Sustainable Materials and Technologies 48 (2026) e01928

Contents lists available at ScienceDirect

Sustainable Materials and Technologies

journal homepage: www.elsevier.com/locate/susmat

3D printing to optimize the dry forming of thermomechanical pulp and chemi-thermomechanical pulp trays for food packaging

Gary Chinga-Carrasco

RISE PFI, Høgskoleringen 6b, 7491 Trondheim, Norway

ARTICLE INFO

Keywords:
Thermoforming
Dry-forming
Wood fibres
Characterization
3D printing
Mechanical properties

ABSTRACT

Environmental concerns over plastic pollution have intensified the search for alternative materials for single-use products, such as trays for food packaging. Dry forming, using wood pulp fibres, is a promising technology for the fabrication of various single-use products. However, the fabrication of trays with relatively complex geometry is challenging. In this study, an approach is introduced where trays are pre-formed in tailored three-dimensional (3D) printed meshes with varying distances between the printed lines in the side walls (1.5 mm, 1.8 mm and 2.0 mm) and bottom (1.0 mm) of the trays. This was expected to facilitate the deposition of wood pulp fibres during formation of a given tray geometry and subsequently yield trays with adequate grammage and mechanical properties. The approach was tested with thermomechanical pulp (TMP) and chemi-thermomechanical pulp fibres (CTMP). Both fibres have similar chemical composition (carbohydrates and lignin), but differed with respect to the structural properties. TMP fibres revealed higher fraction of disrupted fibres and fibrils on the fibre surfaces. These characteristics increased the densification of the TMP trays during thermoforming and thus provided higher mechanical properties, compared with the corresponding CTMP trays. A tray demonstrator was developed, with tray depth of 50 mm and side wall angles of 65°. Thermopressed trays (pressure and temperature of 40 MPa and 200 °C, respectively) yielded strength and modulus of 1–10 MPa and 400–1600 MPa, respectively. The mechanical performance depended on the type of fibre (TMP or CTMP) and on the area of measurement in the trays (side walls or bottom).

1. Introduction

The environmental pollution caused by plastic products has become a global issue. This is mostly due to: i) large amounts of plastic produced worldwide (460 million metric tons/year), ii) limited infrastructure and processes for plastic recyclability, often causing plastic littering (20 million metric ton/year) and iii) poor biodegradability in nature of most plastic products [1]. Consequently, plastic contamination causes major negative effects on land and marine wildlife [1,2].

During the last years it has been a major interest on lignocellulosic fibres as a main component of renewable, biodegradable and recyclable products to replace single-use plastic products [3]. Various types of lignocellulosic fibres have been utilized from e.g. wood and annual plants [4]. Wood pulp fibres are especially interesting as they are produced in large volumes following well-established technologies that improve the efficiency of pulp production [5,6]. Among wood pulp fibres, thermomechanical (TMP) and chemi-thermomechanical pulp (CTMP) are interesting due to their high production yield (more than 90%) and lower prices, compared to e.g. chemical pulps [7].

Wood pulp fibres have been utilized to manufacture e.g., trays, liquid containers, caps, etc. Such products have been rapidly developed based on two main fibre-moulding technologies, i.e., wet-moulding and dry forming. Wet-moulding has been a most utilized technology for production of packaging items [8]. In wet-moulding, fibres are dispersed in water at a given concentration (usually lower than 1%), the fibre suspension is suctioned into a mould, compressed with high pressure and temperature, and dried to consolidate a given three-dimensional product. Cycle times between 30 and 70 s have been stated [9]. Recently, dry forming has gained interest due to the potential benefits of being more environmentally friendly, i.e., the lack of water in the forming process reduces the drying step and thus the energy consumption. Therefore, dry forming requires shorter cycle times (usually less than 10 s). However, lignocellulosic fibres also benefit from the presence of water during the formation and drying processes, as water promotes the formation of hydrogen bonds between fibres [10]. Therefore, the absence of water in dry forming tends to yield 3D thermopressed specimens that are weaker than those formed with wet-moulding [11].

The choice of fibres is important in fibre moulding processes.

E-mail address: gary.chinga.carrasco@rise-pfi.no.

https://doi.org/10.1016/j.susmat.2026.e01928
Received 8 October 2025; Received in revised form 3 February 2026; Accepted 15 February 2026
Available online 20 February 2026

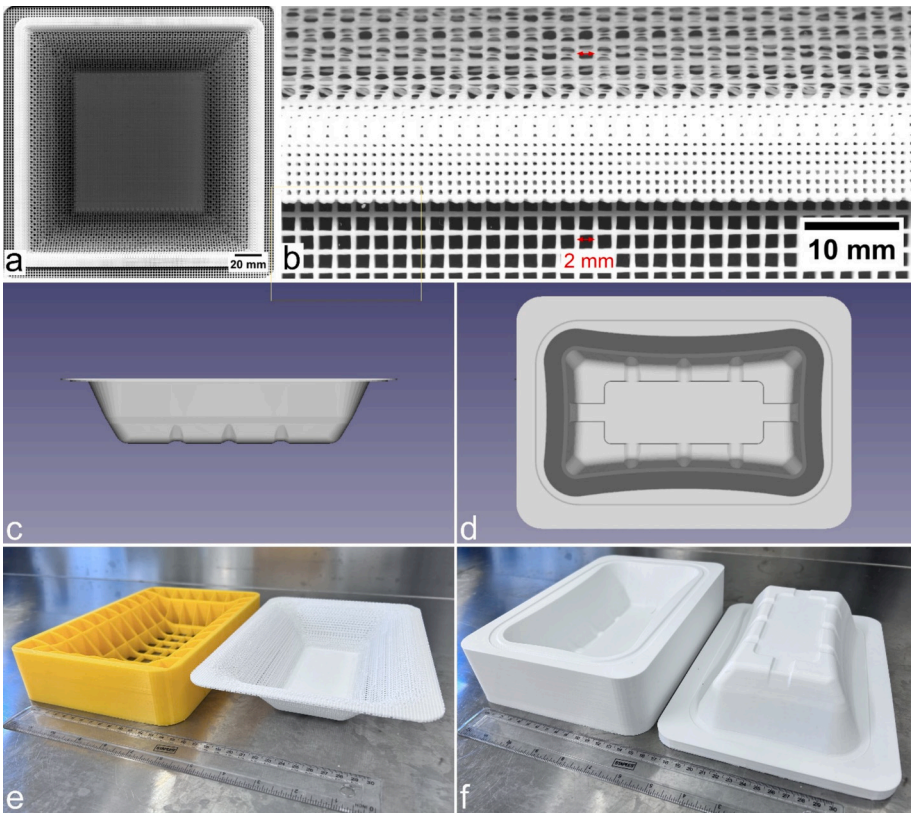

Fig. 1. 3D printed devices for dry-forming and cold-pressing. a) 3D printed mesh for dry forming of relatively simple trays (side walls 30°, with bottom and side wall mesh line distance of 1.0 and 2.0 mm, respectively. b) Magnified area of the 3D printed mesh exemplifying the line distance (red arrow, 2 mm). The upper part corresponds to the side wall and the lower part to the flat edges. c and d) 3D graphical design of a more complex tray with height of 50 mm and side walls of 65°. e) 3D printed mesh support (yellow) and porous mesh (side walls 65°). f) 3D printed moulds for cold-pressing.

Refining affects the fibre wall thickness and the collapse index of TMP fibres [12], and thus the corresponding strength and stiffness [13,14]. On the other hand, CTMP provides bulk and drainability (e.g. Canadian Standard Freeness of >500 ml) [15], which is considered an advantage for wet-moulding. Fines also influence the mechanical properties positively, increasing tensile strength [14,16]. TMP is especially interesting in this respect as this is a high-yield pulp (~95%), that is relatively cheap. In addition TMP offers a fibre morphology that includes thin wall fibres, split fibres and fines [17]. Such fibre morphology may favour the densification of trays during thermoforming and, consequently, the development of appropriate mechanical properties.

Three-dimensional (3D) printing has become a widely used technology for various applications. A range of 3D printing technologies exists, including stereolithography, fused deposition modelling (FDM), selective laser sintering [18]. FDM is a most versatile process, where polymers (e.g. polylactic acid (PLA), acrylonitrile butadiene styrene, high density polyethylene, etc) [18] and biocomposites (e.g. PLA reinforced with natural fibres) [19], are melted and deposited in a controlled process in the x, y and z direction, to form a given 3D shape. FDM is widely used in the hobbyist and home sector due to the low cost, ease of use and affordable desktop printers. FDM has also major potential for rapid prototyping of parts and functional devices with complex geometries and applications in, e.g., biomedicine, construction, automotive, aerospace, acoustics [20].

According to Freville et al. [21], the main limitation with dry forming was the depth of the formed item that was limited to 30 mm. Hence, in this study a new approach was introduced where meshes with varying geometries were 3D printed for a pre-formation step that secured adequate distribution of the fibres in the tray walls and bottom. The pre-forming step was introduced to facilitate the forming of geometries that are higher than 30 mm. The approach was demonstrated with two relevant wood pulps, i.e., TMP and CTMP. The study provides a direct one-to-one comparison between TMP and CTMP, regarding formation, structure and mechanical properties of dry formed tray products.

2. Materials and methods

2.1. Fibre characterization

Picea abies chips and the corresponding TMP fibres were provided by Norske Skog Saugbrugs. The CTMP was a Scandinavian market pulp. The chemical composition and morphology of the pulp fibres were assessed. The carbohydrate composition and lignin content was quantified following the protocols described in NREL/TP-510-42,618 "Determination of Structural Carbohydrates and Lignin in Biomass". The acid soluble and insoluble lignin was quantified according to TAPPI UM 250 and NREL/TP-510-42,618-method, respectively.

A Lorentzen & Wettre Fibre Tester Plus was used to quantify the pulp fibre dimensions in triplicate. The pulp fibres (0.1 g) were dispersed in 300 ml distilled water before measurement. The fibre length (mm), width (μm), fines (length averaged, %), fibril perimeter (%) and fibril area (%) were quantified.

The Canadian Standard Freeness (CSF) of the pulps was measured in duplicate according to ISO 5267-2:2001 standard.

2.2. Scanning electron microscopy and analysis

The pulp fibres (TMP and CTMP) and thermopressed samples (TMP and CTMP trays, bottom and side wall samples) were embedded in epoxy resin for scanning electron microscopy analysis (SEM, Hitachi SU3500), in backscatter electron imaging (BEI) mode. The epoxy-

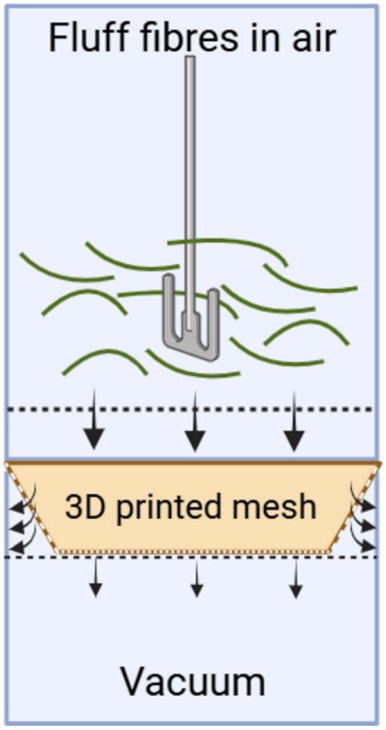

Fig. 2. Schematic representation of a dry forming step.

embedded samples were dried for at least 48 h before grinding and polishing as described by Reme et al. [22]. The samples were coated with carbon before imaging at 100× and 300× magnification. Four images were acquired for each sample, with a resolution of 0.17 μm/pixel (300× magnification). Correspondingly, SEM secondary electron imaging (SEI) was applied to acquire images from the surface of the fibres. The samples were coated with a thin layer of gold before imaging at 300× magnification.

Image processing and analysis was performed on the SEM BEI images, including thresholding, median filtering and binary operators to remove noise particles. The cross-sectional analysis was based on a Euclidean distance transform (EDT), as previously described [23].

2.3. 3D printing of meshes and moulds

The Solidworks software (2023 SP4 version) was used for designing various parts for dry forming, including the meshes, supporting frames and moulds. The geometry of Tray 1 (Fig. 1, upper panel) was relatively simple, i.e., 200 × 200 mm and 30° side wall inclination. Three meshes were 3D printed with varying line distances on the side walls, i.e., 1.5, 1.8 and 2.0 mm (Fig. 1a and b). The mesh size at the bottom of the mesh was 1.0 mm and remained constant. The line distance was defined in the Cura program (version 4.5) by defining the infill pattern and refers to the distance from the centre point of one printed line to another (Fig. 1b). The obtained mesh openings after printing may be influenced by the nozzle dimensions and the printing parts. i.e. more accurate on the flat bottom than on the inclined side walls of the tray mesh (Fig. 1b).

A second tray was designed with dimensions 243 × 156 mm, with 65° side wall inclination (Fig. 1, lower panel). Two meshes were 3D printed for fabricating this tray, i) side wall line distance of 2.0 mm and bottom of 1.0 mm, and ii) side wall line distance of 2.0 mm and solid bottom (no openings).

All the devices were sliced with the Cura program and 3D printed with an UltimaMaker S5 printer, using polylactic acid (PLA) filament (diameter: 2.85 mm) and a nozzle of 0.4 mm. The mesh support, porous mesh and moulds for cold-pressing are presented in Fig. 1.

2.4. Dry forming

The dry pulp fibres (TMP and CTMP) were fluffed with a hammermill at 4500 RPM and using a 5-mm wire opening. The fluffy fibres were introduced to a dry forming apparatus consisting of a forming head, forming table and vacuum box. The size of the forming table was 300 × 300 mm. The 3D printed mesh was placed in the middle of the forming table and was used to collect fibres as a stream of air was maintained from the forming head to the forming table (Fig. 2). The target grammage of the pre-formed samples was 500 g/m^2.

The pre-formed samples (using the meshes exemplified in Fig. 1a and e) were transferred from the 3D printed mesh to 3D printed moulds for cold-pressing (force 50 kN during 1 min). This step was performed to consolidate the pre-formed trays and facilitate the manual transfer of the trays to the hot metal moulds. The metal moulds were manufactured in 7075 aluminium alloy. The moulds were designed so that the bottom and upper edges of the mould parts touched when no fibres were present between them. The trays were thermopressed in the metal moulds using 10, 30 and 40 MPa pressure, during 30 s at 200 °C. This temperature is above the softening temperature of lignin [24], and it was expected that this would contribute to increasing the density and strength of the thermoformed trays.

In a first trial, the formation of the deep trays (depth = 50 mm, Fig. 1c-1f) was divided into two steps: i) a pre-forming step (30 s) with the 3D printed mesh having 2.0 mm side wall line distance and 1.0 mm bottom line distance, and ii) a consolidation step (120 s) with a 3D printed mesh with 2.0 mm side wall line distance and solid bottom (without openings). The second trial was also divided into two steps: i) fibre deposition with the bottom of the mesh completely closed (without pores) and the side walls with mesh line distances that increased gradually from 0 (bottom) to 1.5, 1.8 and 2 mm in the upper part of the side wall and ii) a second deposition step where only the side walls were allowed to collect fibres, i.e., the deposition of fibres on the bottom was blocked by placing a solid 3D printed cup that collected fibres from the central part of the tray. The cup with collected fibres was removed after forming. This was done to force the deposition of fibres on the side walls by the airstream caused by vacuum and limit the deposition of fibres on the bottom of the tray. The trays were thermopressed with 40 MPa (1950 kN), during 30 s.

The temperature of the moulds was 200 °C during all the pressing trials. A LabPro 2000 press (Fontijne, the Netherlands) was used for hot-pressing.

2.5. Characterization of the thermoformed trays

The tray samples were conditioned at 23 °C and 50% relative humidity for at least 24 h before measurements. The thicknesses and densities of the bottom and sides of the trays (TMP and CTMP) were

Table 1
Chemical composition of the chips and wood pulp fibres applied in this study.

Code	Sugars					Lignin	
	Glucose (%)	Xylose (%)	Galactose (%)	Arabinose (%)	Mannose (%)	Acid Insoluble (%)	Acid soluble (%)
Chips	42.91 ± 0.93	5.20 ± 0.20	1.44 ± 0.05	0.75 ± 0.02	11.35 ± 0.94	27.99 ± 0.14	0.55 ± 0.02
TMP	47.50 ± 0.02	5.03 ± 0.28	1.30 ± 0.08	0.61 ± 0.03	12.87 ± 0.92	26.13 ± 0.13	0.52 ± 0.52
CTMP	44.24 ± 1.83	5.41 ± 0.28	2.00 ± 0.13	0.96 ± 0.11	10.94 ± 0.35	26.91 ± 0.02	0.85 ± 0.08

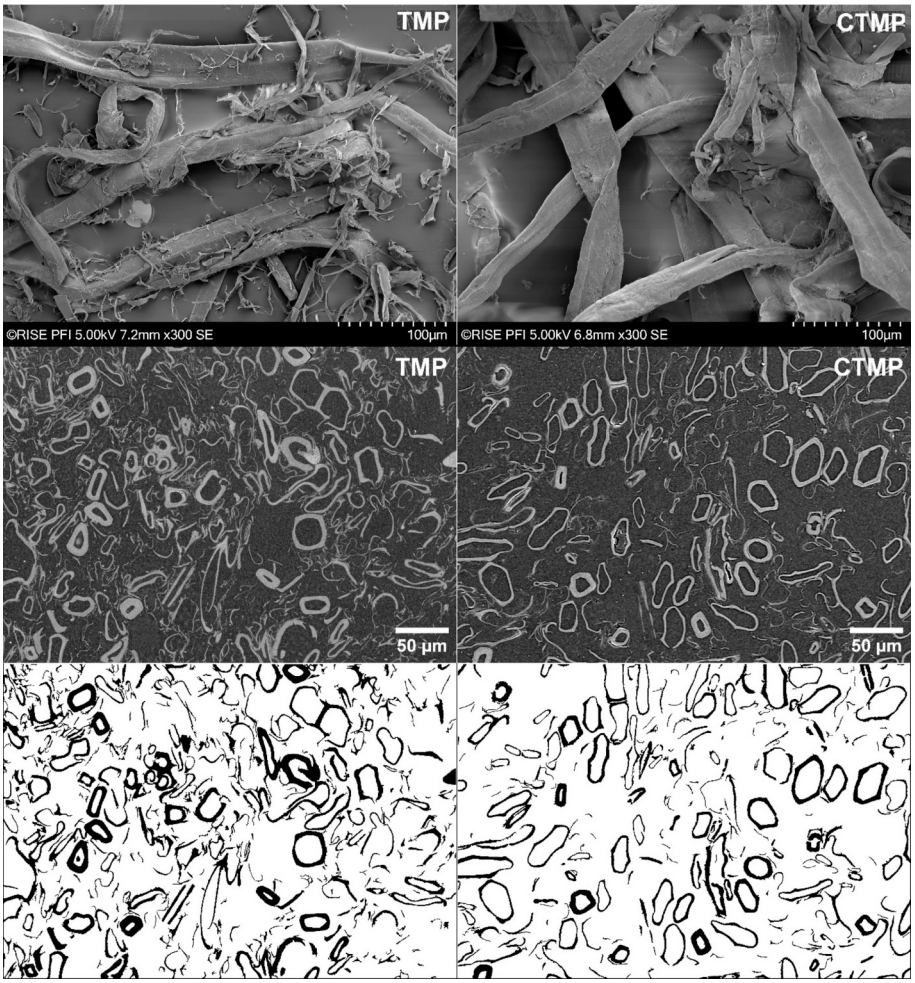

Fig. 3. SEM surface images (upper panel), SEM BEI analysis (middle panel) and the corresponding binarized images (lower panel).

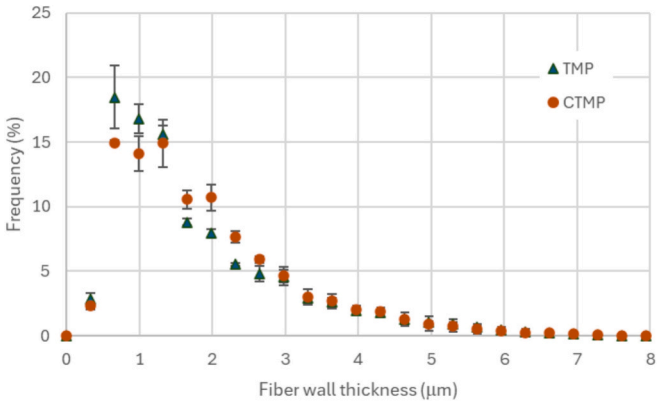

Fig. 4. Quantification of fibre wall thicknesses based on EDT.

quantified, according to ISO 534 Paper and board – Determination of thickness, density and specific volume). Four replicates were undertaken for the bottom and sides of each sample.

A Zmart.Pro universal material tester (Zwick, Germany) was used to assess the mechanical properties (tensile strength, modulus and elongation), following the ISO 1924-3 Paper and board — Determination of tensile properties — Part 3: Constant rate of elongation method (100 mm/min). The width of the assessed samples was 15 mm and the distance between the clamps during tensile testing was 40 mm.

Table 2
Fibre Tester analysis of TMP and CTMP.

Pulp code	Mean length (mm)	Mean width (µm)	Mean fibril area (%)	Mean fibril perimeter (%)	Fines (%)
TMP	1.38 ± 0.03	33.13 ± 0.21	10.43 ± 0.38	34.33 ± 0.87	45.83 ± 0.70
TMP-fluffed	1.25 ± 0.01	32.27 ± 0.06	5.97 ± 0.38	20.50 ± 0.96	47.87 ± 0.32
CTMP	1.50 ± 0.02	35.77 ± 0.12	4.17 ± 0.15	16.77 ± 0.49	58.07 ± 0.85
CTMP-fluffed	1.45 ± 0.01	36.37 ± 0.31	3.30 ± 0.17	13.50 ± 0.36	54.80 ± 0.72

3. Results and discussion

3.1. Fibre characteristics

The chemical composition of the *Picea abies* chips and mechanical pulp fibres (TMP and CTMP) are given in Table 1. There are no major differences between the chips and the two pulp fibres, having similar content of sugars and lignin. The carbohydrate composition and lignin content are within the levels previously reported for wood from *Picea abies,* e.g. *glucose between 42 and 48% and lignin between 26 and 28%* [25–27], which confirms the obtained results.

The TMP process applies pressurized steam to facilitate the refining by softening the lignin. Some 2000 kWh/ton is typically consumed

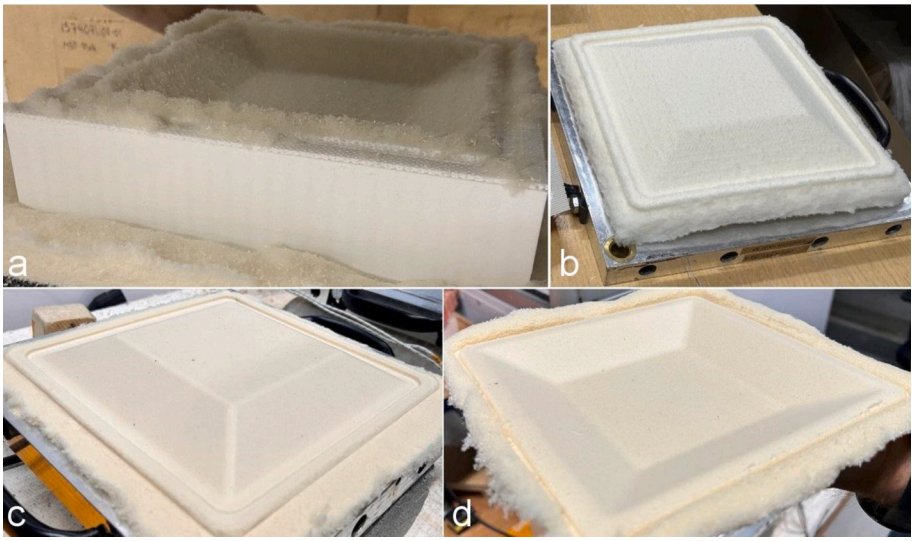

Fig. 5. Formation of trays. a) Formation step, fibres deposited on the 3D printed mesh. b) Pre-formed tray transferred to the upper metal plate. c) and d) Bottom and top side of the tray after thermopressing.

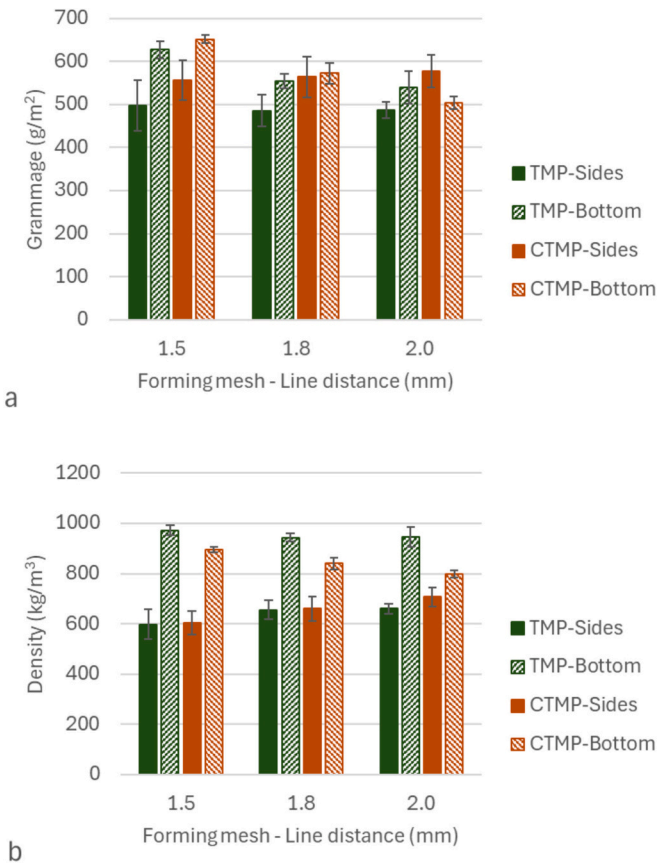

Fig. 6. Grammage (a) and density (b) of trays as a function of the mesh line distance. The pressure during thermopressing was 10 MPa.

during the TMP process [28]. The TMP fibres used in this study are from the reject press and it is estimated that some 1600 kWh/ton was consumed during refining. On the other hand, Na_2SO_3 is used to impregnate the pulp and decrease the softening temperature of lignin during the CTMP process. The sulfonation improves the separation of fibres thus obtaining bulky pulp at relatively low energy consumption [29]. The increase of the sulfonate content from 0 to 0.3% has increased the tensile index of the pulps from ~43 to ~51 Nm/g, for pulp refined at 1950 kWh/ton [30].

As expected, differences were quantified between the TMP and CTMP fibres. The TMP fibres were typically more disrupted than the CTMP fibres, i.e., the TMP contained a larger fraction of split fibres and fibrillar material compared to the bulkier and more intact CTMP fibres (Fig. 3). The CSF of the TMP and CTMP were 424 ± 5.7 and 580 ± 1.4, respectively. The SEM surface analysis (Fig. 3, upper panel) shows clear differences between the TMP and CTMP fibres. In addition to being more disrupted, the TMP fibres appear more fibrillated with notorious fibrils arising from the fibre surface, while the CTMP fibres seem smoother. SEM cross-sectional analysis confirmed the larger fraction of disrupted fibres and apparently fibrillar fines compared to the CTMP. The frequency of thin TMP fibre wall thicknesses (<1 μm) was higher than in the CTMP. On the other hand, the CTMP had a higher frequency of fibres with relatively thicker fibre walls, i.e., thickness between roughly 1.5 and 3 μm (Fig. 4). The morphology of the CTMP fibres was also confirmed by the Fibre Tester analysis. CTMP contained longer and wider fibres, with a lower fraction of fibrils, compared to the TMP (Table 2). However, a larger fraction of fines was quantified in the CTMP (55%) than in the TMP (48%). Although, the fluffing of the pulps didn't affect the fibre morphology considerably, some minor changes were detected, i.e., the fluffing reduced the fibre length and fibril fraction and roughly maintained the width. The quantification also indicated that the fines content increased for the TMP and was somewhat reduced for the CTMP (Table 2).

3.2. *Forming and characterization of trays with side wall inclination of 30°*

Dry forming is usually based on flat fluffy mats that are compressed into a pre-defined 3D shape. According to Freville et al. [1], the production of 3D shapes by dry forming was limited to a depth of 30 mm in 2023. This was probably due to a relatively poor conformation of flat fibre mats in deep 3D shaped moulds and the high pressures applied during a short period of time.

The approach introduced in this study demonstrates the advantages of 3D printing, where meshes for pre-forming trays can be designed to collect fibres differently, by the walls and by the bottom of the trays. This could help to compensate for the differences in grammage, density and mechanical properties of deep trays for food packaging. A relatively simple tray was used in this part of the study to demonstrate the concept

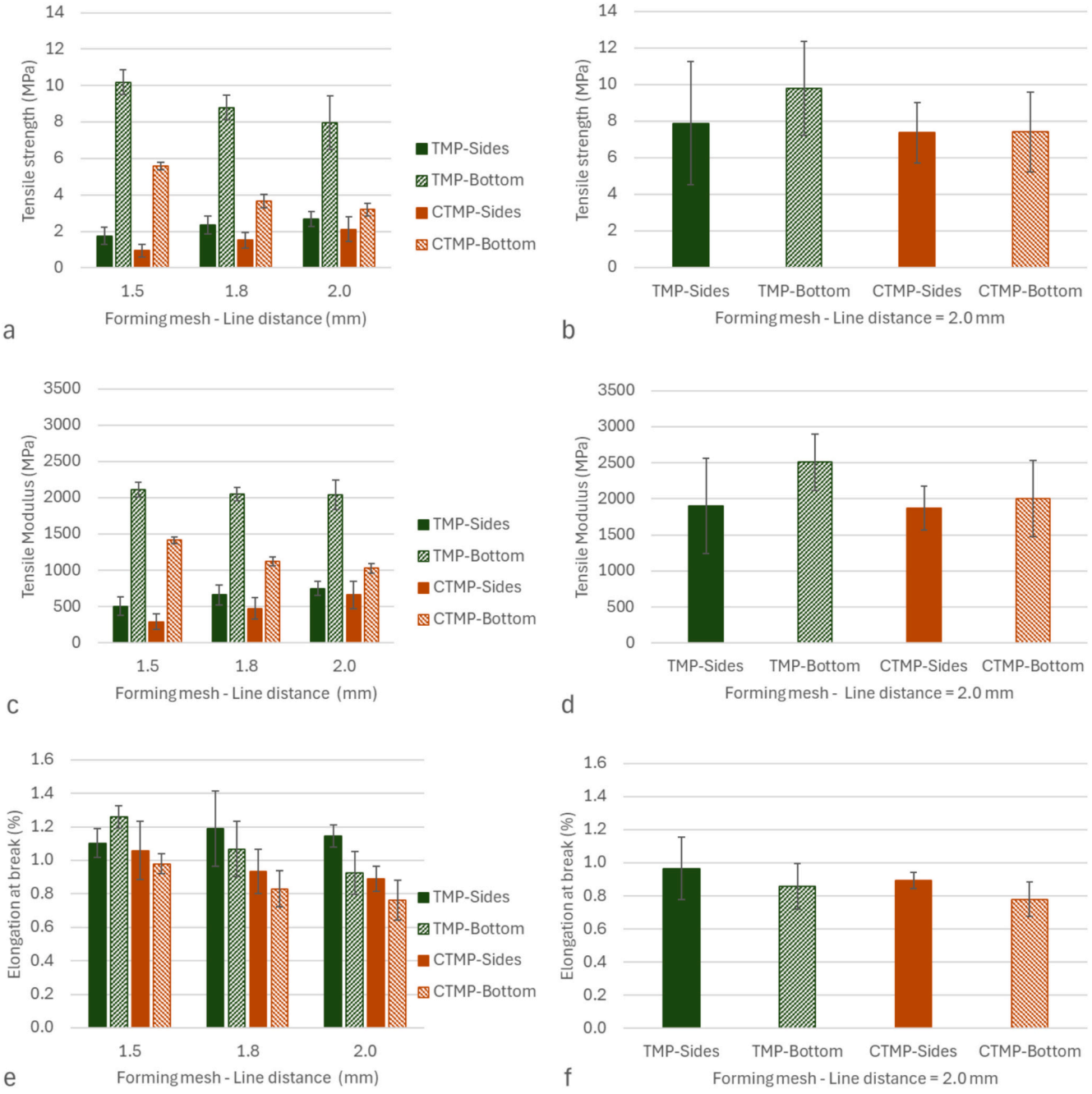

Fig. 7. Mechanical properties of trays as a function of the mesh line distance and pressure (a, c and e). The pressure during thermo-pressing was 10 MPa, (a, c and e) and 30 MPa (b, d and f). The side wall line distance was fixed at 2.0 mm for the samples pressed at 30 MPa.

of differential fibre deposition in a 3D shaped mesh (Fig. 5). The concept is based on i) depositing fluff fibres directly on a 3D printed mesh, ii) the fluffy pre-formed tray is transferred to metal plates and iii) the tray is thermopressed. The TMP and CTMP fibres applied in this study are mechanical pulp, which contain roughly 27% lignin (Table 1). Considering the lignin content, the temperature applied during hot-pressing was chosen to be 200 °C as it was expected that this temperature would secure a higher densification and mechanical strength of the mechanical pulps [31]. The onset of thermal degradation of CTMP has been reported to be 264 °C [32].

The obtained grammage of the trays varied between 500 and 650 g/m^2, being the grammage of the bottom of the trays generally higher than those of the side walls (Fig. 6a). The difference in grammage between the bottom and sides of the trays was largest when using the mesh with smallest line distance (1.5 mm). A similar trend was measured for the densities of the bottom and side walls of the trays, as a function of mesh line distance (Fig. 6b). The difference between the bottom and the side walls was reduced as the line distance of the sides was larger, while maintaining the same line distance at the bottom (1.0 mm). This behaviour was expected as widening the line distance in the side walls (from 1.5 to 2 mm) would increase the pore size of the mesh, reduce the resistance to air-flow and thus increase the deposition of fibres on the side walls more rapidly, compared to the bottom. Although, a decrease of grammage was quantified on the bottom of both trays (TMP and CTMP), the grammage on the sides of the corresponding trays was relatively constant (Fig. 6a). Moreover, despite higher grammage on the sides of the CTMP trays than on the TMP trays, the densities between both series (TMP and CTMP, side walls) were similar. Additionally, the

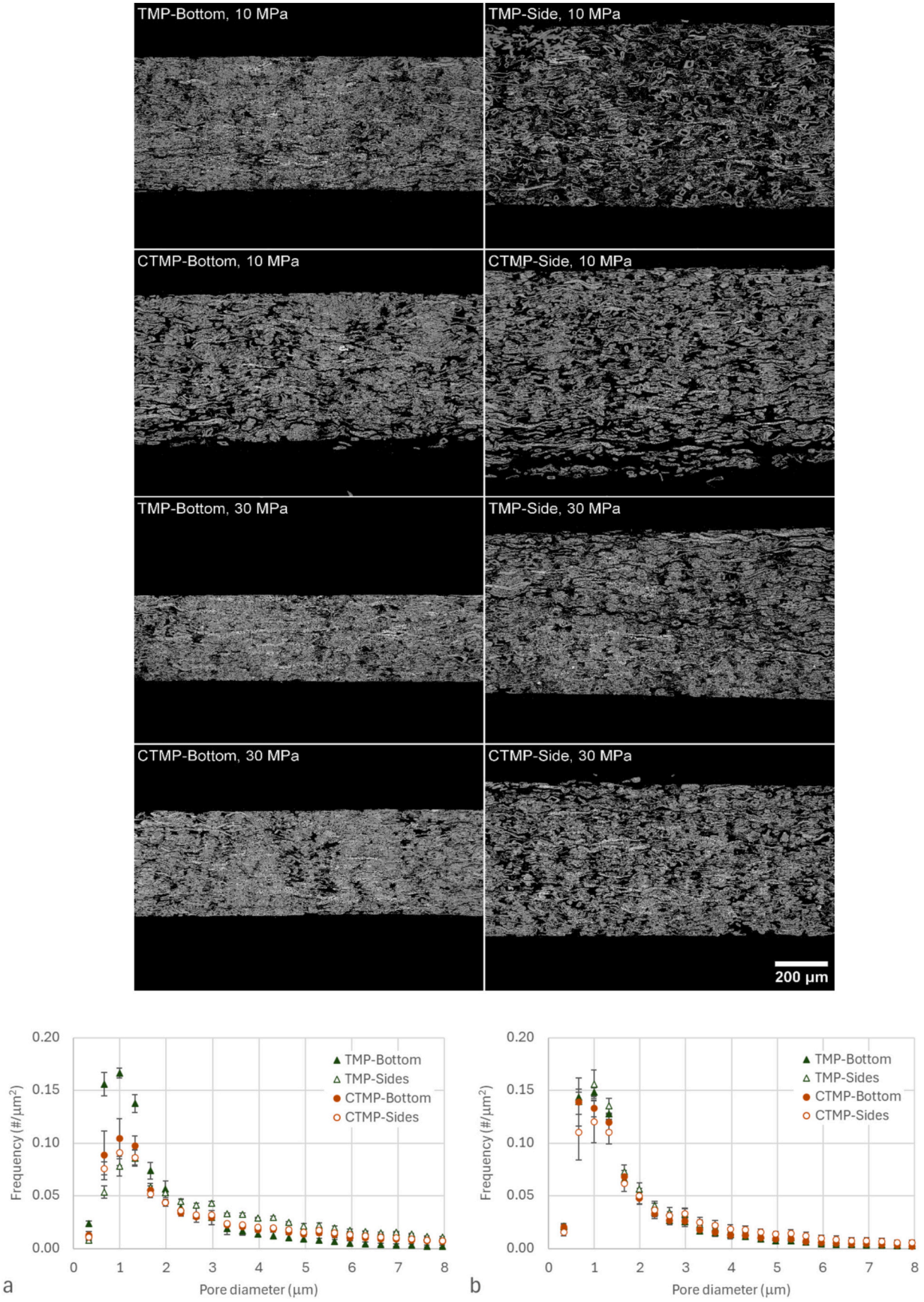

Fig. 8. Upper panel) SEM cross-sectional images of thermopressed samples. Lower panel) Pore diameters of samples from the sides and bottom of thermopressed TMP and CTMP trays. Pressure during thermopressing was 10 MPa (a) and 30 MPa (b). The background of the images was removed for better visualization. All the images were acquired with 100× magnification.

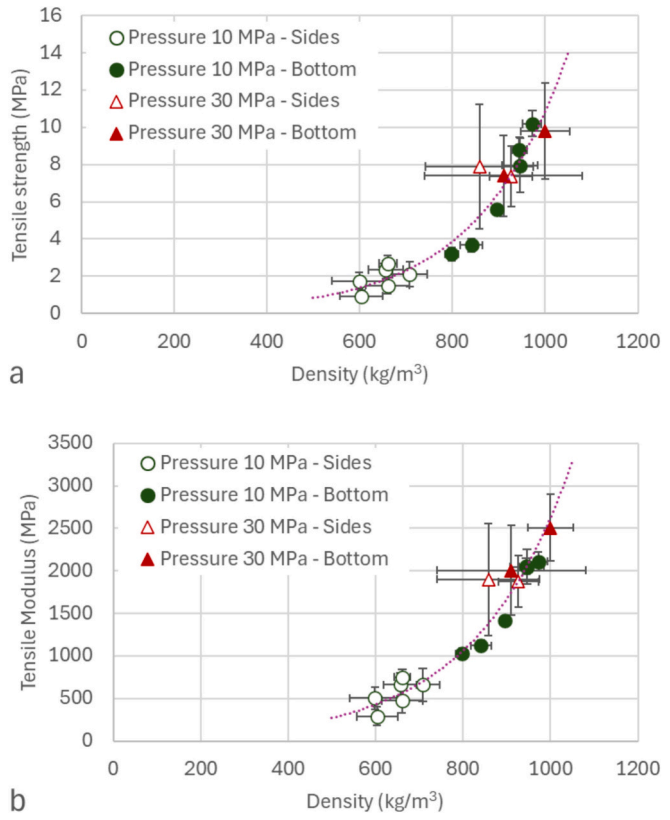

Fig. 9. Relationship between density and strength (a), and modulus (b).

densities on the bottom of the TMP and CTMP trays were consequently higher than on the side walls, and the densities of the bottom decreased as the side walls line distance increased (Fig. 6b).

It has been demonstrated that increased nip temperature (up to 200 °C) during hot-pressing in a rotating cylinder press, increased the density and tensile strength of CTMP and TMP sheets [33]. In this study, the tensile properties of the trays were affected by the densities at the corresponding bottom and side walls (Fig. 7). A clear tendency was quantified, where the tensile strength and modulus of the side walls increased as the line distance of the forming mesh sides increased from 1.5 to 2 mm (Fig. 7a, c, e). The tensile properties of the bottom areas decreased accordingly, reducing the differences between the bottom and side walls. Further, the tensile strength and modulus of the TMP were higher than the CTMP fibres, irrespective of the area of assessment (bottom or side walls). This behaviour is partly attributed to the differences regarding fibre morphology, i.e. the TMP fibres are more disrupted and with a larger fraction of surface fibrils (Fig. 3 and Table 2) compared to the CTMP fibres which are more intact and stiffer. According to Pettersson et al. [14], bending stiffness can be reduced by making the fibres thinner, which is the case with TMP fibres (Fig. 3). Additionally, it has been demonstrated that split fibres, fibrils, and fines affected the z-strength and tensile index of laboratory TMP sheets [34]. Hence, the split fibres in TMP are expected to facilitate the densification of the fibre network during pressing and the larger fraction of external fibrillation of TMP fibres may contribute to the mechanical interlocking of neighbouring fibres, thus increasing the strength [35,36].

It has been reported that wet-moulding provides better mechanical properties than dry forming [11]. The absence of water during thermoforming limits the inter-fibre bonding [37], thus reducing the tensile properties. The tensile strength achieved in this part of the study was relatively low (2–10 MPa). As an attempt to improve the mechanical performance of the trays, a new set of samples were manufactured, using the same temperature but increasing the pressure from 10 MPa to 30 MPa. The results confirmed that the pressure has a considerable effect on the strength and modulus (Fig. 7b, d, f). This was especially the case on the side walls that increased from roughly 2 MPa to 8 MPa (strength) and from roughly 500 MPa to 2000 MPa (modulus). Additionally, the differences between the bottom and side walls of this specific tray (side wall angle = 30°) were reduced considerably (Fig. 7).

Increasing the pressure (from 10 MPa to 30 MPa) led to a compaction of the fibre network, increasing the density and reducing the porosity of the thermoformed samples. As stated above, the density has a significant effect on the mechanical properties. Low density indicates fibre networks with high porosity, and consequently low fibre-fibre bondings. Using kraft fibres, Upadhyay et al. [38] demonstrated that shorter fibres and increased fines content led to higher density, which according to the authors improved fibre web consolidation and a reduction in porosity. Joelsson et al. [33] demonstrated that a large fraction of fines in TMP contributed to denser TMP sheets compared to CTMP. In the present study, SEM cross-sectional analysis revealed differences between the relatively densified bottom structures and fluffy and less dense side walls (Fig. 8). The measurements from the TMP-Bottom sample showed a relatively high occurrence of small pores, indicating a denser structure. Such compacted structure obviously increases the fibre-fibre bonding, probably facilitated by a larger fraction of fibrils (Fig. 3, Fig. 4 and Table 2). This seems to confirm the higher tensile strength and modulus obtained for the TMP-Bottom samples compared to the other series (Fig. 7). The presence of collapsible fibrils in TMP has been reported to improve the bonded surface area between fibres and the tensile strength of handsheets [39], which provides support for the results of the present study. Additionally, it has been demonstrated that mechanical properties (yield strength and Young's modulus) increased probably caused by fibril aggregate interactions in fibre-fibre bondings, promoted by pressing temperature [40]. According to Asta et al. [41], high-density sheets of CTMP fibres (1000 kg/m^3) were closely packed, which increased the concentration of fibre-fibre joints and the stiffness and tensile strength. The high-density sheets had extensive fibre breakage after tensile testing, i.e., fibre pull-out was reduced as revealed by SEM inspection of fracture areas [41]. These studies [39–41], have provided additional evidence that pulp components (e.g. fibre cross-sectional shape, fibrils, fines) influence the formation of well-connected networks that are densified under high-pressure and temperature, resulting in enhanced mechanical properties.

In this study, SEM analysis also revealed the effect of increased pressure during thermopressing (Fig. 8), i.e., the higher pressure (30 MPa) led to a further compaction of the fibre network and thus lower porosity, reduced thickness and higher densities (Supplementary, Table S1.). Numerical data supported these observations. Quantification of the pore diameters showed a large occurrence of pores with diameters less than roughly 1.5 μm for the samples TMP – Bottom and CTMP – Bottom, compared to the corresponding side wall samples, which had a larger occurrence of pore diameters larger than 3 μm (Fig. 8, lower panel). Increasing the pressure from 10 MPa to 30 MPa reduced the differences between the samples regarding the pore sizes. This indicates that higher pressure may contribute to overcoming the differences related to the fibre morphology between the TMP and CTMP, and the differences between the corresponding tray areas (bottom or side walls).

It is obviously a clear relationship between the densities of the samples and the mechanical properties (Fig. 9). As reported above, there is a substantial difference between the densities of the side walls and the bottom of the trays (pressed with 10 MPa). These differences are reduced as the densities increase. The corresponding tensile strength developed from roughly 1–2 MPa to 10 MPa as the densities approaches 1000 kg/m^3. A direct correlation demonstrates that the development of strength and modulus had a non-linear evolution (Fig. 9). Orgéas et al. [42] demonstrated that the elastic moduli of low-density fibre networks (densities between ~300 and 700 kg/m^3) increased as a power-law function of the fibre content. Furthermore, a rapid increase in tensile strength of Eucalyptus handsheets at relatively high densities (600–900 kg/m^3) has been reported previously [43]. Additional testing in this

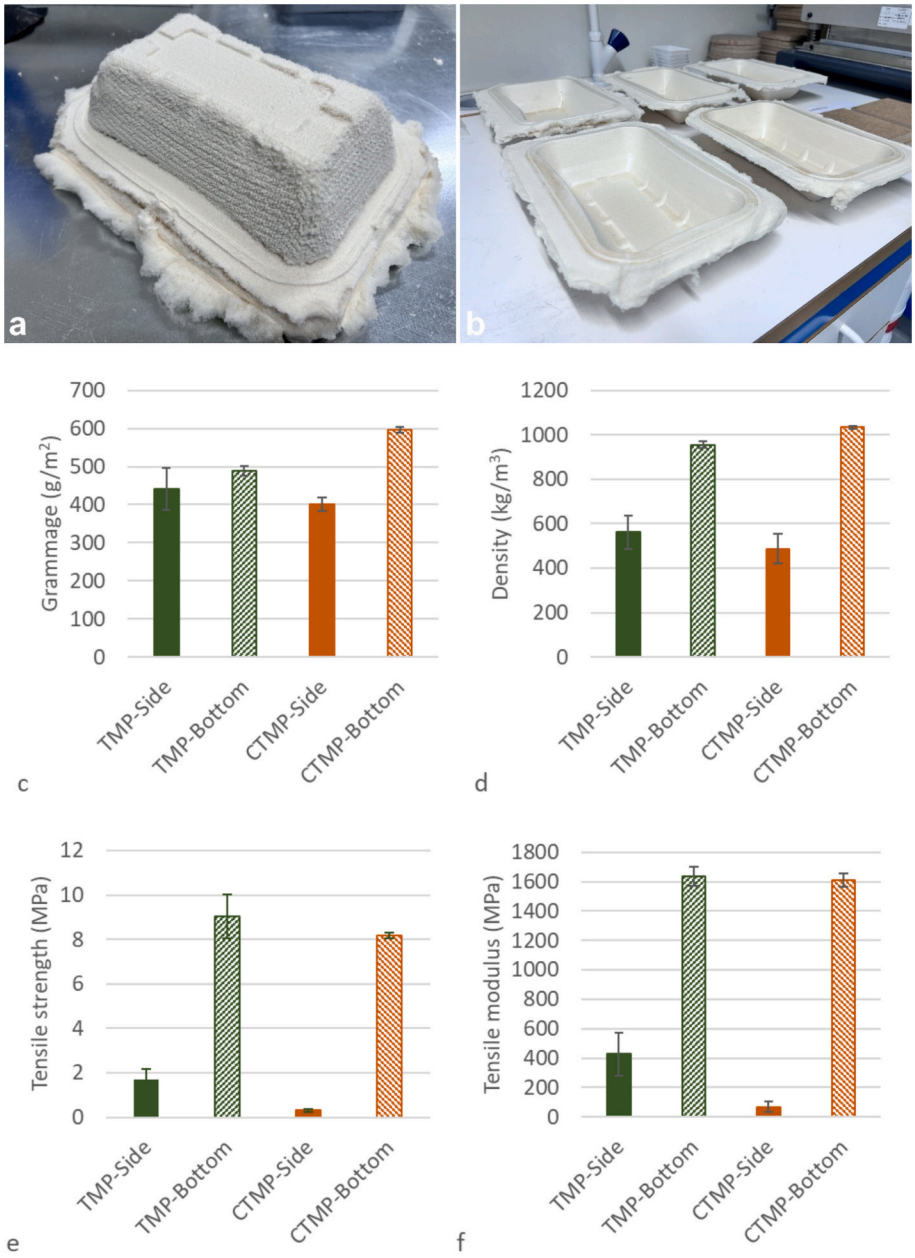

Fig. 10. Formation of a 50 mm deep TMP tray. a) The underside of a pre-formed tray. b) Trays after thermopressing. c) Grammage. d) Density. e) Tensile strength. f) Tensile modulus.

Table 3
Characteristics of TMP trays.

TMP tray	Basis weight (g/m^2)	Density (kg/m^3)	Tensile strength (MPa)	Modulus (MPa)	Elongation (%)
Side wall	636.5	721.6	4.3 ± 0.7	1077 ± 154	0.8 ± 0.0
Bottom	453.6	817.9	4.2 ± 1.9	1110 ± 405	0.8 ± 0.0

study confirmed the non-linear evolution of strength and modulus, achieving levels of approximately 50 MPa and 5000 MPa, respectively, as the density approached 1300 kg/m^3 (Supplementary information Fig. S1).

3.3. Forming and characterization of deep trays (50 mm) and side wall inclination of 65°

The approach developed in this study was tested in the fabrication of more complex tray geometries, with deep and steep side walls (depth = 50 mm, angle = 65°) (Fig. 10). Using a mesh geometry of 1.0 mm (bottom) and 2.0 mm (side walls) yielded pre-formed trays with apparent good distribution of fibres. However, preliminary assessment demonstrated large differences between the side walls and bottom of the trays regarding density and mechanical properties. This was attributed to large grammage differences. In order to compensate for different grammage between the bottom and side walls the formation of this complex 3D shape was divided into two steps: i) a short period of formation (30 s) using the 3D printed mesh with 2 mm side wall line distance and 1.0 mm bottom line distance and ii) a more extensive consolidation step (120 s) with a 3D printed mesh having 2 mm side wall line distance and solid bottom (without openings). Although, this

sequence yielded a more homogeneous distribution of fibres in the side walls and bottom of the TMP trays (Fig. 10c), the grammage of the CTMP-Side and CTMP-bottom differed. After fluffing the CTMP fibres were more dispersed and fluffy, compared to the TMP. This caused that most of the CTMP fibres were deposited during the first step of formation (30 s). On the other hand, approximately equal amounts of TMP fibres were deposited on the mesh during the first and second step of formation, which explain the more homogeneous distribution of fibres between the side walls and bottom (approx. 500 g/m^2).

Note that the testing confirmed the better mechanical properties achieved with TMP compared to the CTMP fibres (Fig. 10e and f). However, there were large differences regarding mechanical properties between the bottom and side walls. As demonstrated above, the tensile strength and modulus of the trays depend on the achieved density (Fig. 9 and Supplementary information Fig. S1). However, the different densities achieved on the side walls and bottom of the trays are due to the different local pressures that were applied. The pressure (P) on a local surface depends on the inclination of the surface. In this case a pressure of 40 MPa on the bottom of the tray (horizontal surface) would correspond to a local pressure of 16.9 MPa on the side walls that are inclined 65° ($P_{side} = P_{bottom}$*cos(α) [44]). Since the pressure at the side walls is less than at the bottom, it is expected that more mass would be necessary in the side walls to obtain the same density as in the bottom, and potentially achieve similar mechanical properties. Based on the measurement of the side walls and bottom of eight trays (Fig. 10) pressed at 40 MPa (Supplementary information Fig. S2), it was estimated that a grammage of approximately 850 g/m^2 would be required to achieve a density of 1000 kg/m^3 (in the side walls), and potentially achieve mechanical properties similar to those obtained at the bottom of the tray.

As an attempt to increase the mechanical properties of the side walls and considering TMP as the best performing pulp in this study, new trays were manufactured. The new strategy was divided into two steps: i) a fibre deposition step with the bottom of the mesh completely closed (without pores) and the side walls of the mesh with distances between lines that increased gradually from 0 (bottom) to 1.5, 1.8 and 2 mm in the upper part of the side wall and ii) a second deposition step where only the side walls were allowed to collect fibres. This approach secured a grammage of some 450 g/m^2 on the bottom and about 637 g/m^2 on the side walls. After pressing the density was 818 and 722 kg/m^3, respectively, providing a similar tensile strength and modulus for the bottom and side walls. Although, the strength is relatively low, decent stiffness levels were achieved (~1100 MPa) for the bottom and side walls (Table 3). This indicates that the mechanical properties of dry-formed trays can be controlled by differential fibre deposition, to achieve similar mechanical performance in the bottom and side walls.

4. Conclusion

Meshes with varying distances between the printed lines were designed and 3D printed for dry forming of trays for food packaging. The 3D meshes were composed of side walls with more open structure compared to the bottom. The approach was tested with trays made of TMP and CTMP fibres, that were pressed with different pressures (10, 30 and 40 MPa) depending on the tray design. Trays made of TMP showed better mechanical properties than CTMP. This was due to the TMP fibre morphology, i.e. more collapsed and split fibres and beneficial fine material that favoured the densification of the trays. Denser structures indicated reduced thickness, porosity and more fibre-fibre bondings which are expected to promote higher tensile strength. The study demonstrated that appropriate geometry of 3D printed meshes is beneficial for manufacturing trays with adequate grammage and density at the side walls and bottom of the trays. Meshes printed with various geometries (distances between 3D printed lines) in the bottom and side walls demonstrated potential in directing the fibres to the bottom and side walls differently in order to control the grammage, thickness, densities of the various parts of the trays. This approach yielded trays with similar mechanical performance in the bottom and side walls.

CRediT authorship contribution statement

Gary Chinga-Carrasco: Writing – review & editing, Writing – original draft, Visualization, Software, Resources, Project administration, Methodology, Investigation, Funding acquisition, Formal analysis, Data curation, Conceptualization.

Declaration of competing interest

The author declares that he has no known competing financial interests or personal relationships that could have appeared to influence the work reported in this paper.

Acknowledgements

The author would like to thank Steinar Seehuus, Berit Leinsvang, Ingebjørg Leirset, Johnny K. Melbø and Kenneth Aasarød from RISE PFI, for skilful laboratory work. This work was supported by funding from the Circular Bio-based Europe (CBE) Joint Undertaking and its members under Grant agreement No 101112521 (REDYSIGN Project).

Appendix A. Supplementary data

Supplementary data to this article can be found online at https://doi.org/10.1016/j.susmat.2026.e01928.

Data availability

Data will be made available on request.

References

[1] Nature, I.U.f.C.o, Plastic Pollution [cited 2025 July 28th, 2025]; Available from: https://iucn.org/resources/issues-brief/plastic-pollution, 2024.
[2] E. Jeong, J.-Y. Lee, M. Redwan, Animal exposure to microplastics and health effects: a review, Emerg. Contam. 10 (4) (2024) 100369.
[3] Y. Su, B. Yang, J. Liu, B. Sun, C. Cao, X. Zou, R. Lutes, Z. He, Prospects for replacement of some plastics in packaging with lignocellulose materials: a brief review, BioResources 13 (2) (2018) 4550–4576.
[4] K.E. Semple, et al., Moulded pulp fibers for disposable food packaging: a state-of-the-art review, Food Packag. Shelf Life 33 (2022) 100908.
[5] L. Kong, A. Hasanbeigi, L. Price, Assessment of emerging energy-efficiency technologies for the pulp and paper industry: a technical review, J. Clean. Prod. 122 (2016) 5–28.
[6] Technology, P.a.P, Sustainable Sourcing of Wood Fiber: Meeting Environmental Goals in Pulp Production [cited 2025 July 28th, 2025]; Available from: https://www.pulpandpaper-technology.com/articles/sustainable-sourcing-of-wood-fiber-meeting-environmental-goals-in-pulp-production, 2025.
[7] W.P. Mill, Chemical Pulping Vs. MEchanical Pulping: Key Differences [cited 2025 July 27th, 2025]; Available from: https://worldpapermill.com/chemical-vs-mechanical-pulping/, 2025.
[8] M. Debnath, R. Sarder, L. Pal, M.A. Hubbe, Molded pulp products for sustainable packaging: production rate challenges and product opportunities, BioRessources 17 (2022) 2810–2870.
[9] Yangi, Comparative Analysis: Wet Molding Vs. Dry Forming (Dry Molding) [cited 2025 April 24th]; Available from: https://www.yangi.se/news/comparative-analysis-wet-molding-vs-dry-molding-dry-forming, 2025.
[10] P.D.M. Przybysz, M.A. Kucner, K. Przybysz, K. Przybysz Buzała, Contribution of hydrogen bonds to paper strength properties, PloS One 11 (5) (2016) e0155809.
[11] E. Pasquier, et al., Effect of raw material and process conditions during the dry forming of CTMP fibers for molded pulp products, J. Nat. Fibers 21 (1) (2024) 2409890.
[12] K.A. Kure, The alteration of the wood fibres in refining, in: Proceedings 1997 International Mechanical Pulping Conference, 1997, pp. 137–150.
[13] R. Ferritsius, S.R. Österling, O. Ferritsius, Mechanical pulping: development of TMP fibers in LC- and HC- refining, Nord. Pulp Pap. Res. J. 27 (5) (2012) 860–871.
[14] G. Pettersson, et al., Aspects on bond strength in sheet structures from TMP and CTMP – a review, Nord. Pulp Pap. Res. J. 36 (2) (2021) 177–213.
[15] J.-E. Berg, et al., Refining gentleness – a key to bulky CTMP, Nord. Pulp Pap. Res. J. 37 (2) (2022) 349–355.
[16] J. Sirviö, I. Nurminen, Systematic changes in paper properties caused by fines, Pulp Pap. Can. 105 (8) (2004) 39–42.
[17] K.A.a.D. Kure, G., Development of structural fibre properties in high intensity refining, Pulp Pap. Can. 99 (7) (1998) 59–63.

[18] A. Jandyal, et al., 3D printing – a review of processes, materials and applications in industry 4.0, Sustain. Operat. Comp. 3 (2022) 33–42.
[19] C. Zarna, et al., Reinforcement ability of lignocellulosic components in biocomposites and their 3D printed applications – a review, Composites C 6 (2021) 100171.
[20] A. Cano-Vicent, et al., Fused deposition modelling: current status, methodology, applications and future prospects, Addit. Manuf. 47 (2021) 102378.
[21] E. Freville, et al., Novel technologies for producing tridimensional cellulosic materials for packaging: a review, Carbohydr. Polym. 342 (2024) 122413.
[22] P.A. Reme, P.O. Johnsen, T. Helle, Assessment of fibretransverse dimensions using SEM and image analysis, J. Pulp Pap. Sci. 28 (4) (2002) 122–128.
[23] G. Chinga, O. Solheim, K. Mörseburg, Cross-sectional dimensions of fiber and pore networks based on Euclidean distance maps, Nord. Pulp Pap. Res. J. 22 (4) (2007) 500–507.
[24] S. Norgren, G. Pettersson, H. Höglund, Strong paper from spruce CTMP – part II: effect of pressing at nip press temperatures above the lignin softening temperature, Nord. Pulp Pap. Res. J. 33 (1) (2018) 142–149.
[25] Z. Wang, et al., Chemical and structural factors influencing enzymatic saccharification of wood from aspen, birch and spruce, Biomass Bioenergy 109 (2018) 125–134.
[26] D.M. Neiva, et al., An integrated characterization of Picea abies industrial bark regarding chemical composition, thermal properties and polar extracts activity, PloS One 13 (11) (2018) e0208270.
[27] I. Čabalová, et al., Chemical and morphological composition of Norway spruce wood (Picea abies, L.) in the dependence of its storage, Polymers (Basel) 13 (10) (2021).
[28] A. Ghose, G. Chinga-Carrasco, Environmental aspects of Norwegian production of pulp fibres and printing paper, J. Clean. Prod. 57 (2013) 293–301.
[29] H. Rahman, P. Engstrand, E. Persson, S. An, B. Norlin, F. Zeeshan, T. Granfeldt, Development of improved CTMP with even sulphonate distribution at fibre level using XRF analysis, in: D. Coffin, W. Batchelor (Eds.), 17th Fundamental Research Symposium, Cambridge, 2022, pp. 3–11.
[30] N. Nelson, A photometric adaptation of the Somogyi method for the determination of glucose, J. Biol. Chem. 153 (2) (1944) 375–380.
[31] L. Wågberg, et al., The build-up of polyelectrolyte multilayers of microfibrillated cellulose and cationic polyelectrolytes, Langmuir 24 (3) (2008) 784–795.
[32] E. Pasquier, R. Skunde, J. Ruwoldt, Influence of temperature and pressure during thermoforming of softwood pulp, J. Bioresour. Bioprod. 8 (4) (2023) 408–420.
[33] T. Joelsson, et al., High strength paper from high yield pulps by means of hot-pressing, Nord. Pulp Pap. Res. J. 35 (2) (2020) 195–204.
[34] C. Sandberg, Fibre development in an intensified mechanical pulping process, Holzforschung 75 (9) (2021) 824–837.
[35] H.R. Motamedian, A.E. Halilovic, A. Kulachenko, Mechanisms of strength and stiffness improvement of paper after PFI refining with a focus on the effect of fines, Cellulose 26 (6) (2019) 4099–4124.
[36] U.a.S. Hirn, R., Fiber-fiber bond formation and failure: Mechanisms and analytical techniques, in: Advances in Pulp and Paper Research, 2017. Oxford.
[37] U. Hirn, R. Schennach, Comprehensive analysis of individual pulp fiber bonds quantifies the mechanisms of fiber bonding in paper, Sci. Rep. 5 (1) (2015) 10503.
[38] A. Upadhyay, L. Lucia, L. Pal, Harnessing total chemical-free paper and packaging materials barrier properties by mechanical modification of cellulosic fibers for food security and environmental sustainability, Appl. Mater. Today 35 (2023) 101973.
[39] B. Alince, J. Porubská, T.G.M. van de Ven, Effect of model and fractionated tmp fines on sheet properties, in: The Science of Papermaking, Trans. of the XIIth Fund. Res. Symp. Oxford, FRC, Manchester, 2001.
[40] H. Nilsson, et al., A non-solvent approach for high-stiffness all-cellulose biocomposites based on pure wood cellulose, Compos. Sci. Technol. 70 (12) (2010) 1704–1712.
[41] N. Asta, et al., Influence of density and chemical additives on paper mechanical properties, Cellulose 31 (9) (2024) 5809–5822.
[42] L. Orgéas, et al., On the role of fibre bonds on the elasticity of low-density papers: a micro-mechanical approach, Cellulose 28 (15) (2021) 9919–9941.
[43] I. Pulkkinen, J. Fiskari, V. Alopaeus, New model for predicting tensile strength and density of eucalyptus handsheets based on an activation parameter calculated from fiber distribution characteristics, Holzforschung 64 (2) (2010) 201–209.
[44] H.M. Beakawi Al-Hashemi, O.S. Baghabra Al-Amoudi, A review on the angle of repose of granular materials, Powder Technol. 330 (2018) 397–417.